Mutational Analysis of the Phototransduction Pathway of *Chlamydomonas reinhardtii*

Gregory J. Pazour,* Oleg A. Sineshchekov,*‡ and George B. Witman*

*Worcester Foundation for Biomedical Research, Shrewsbury, Massachusetts 01545; and ‡Biology Department, Moscow State University, 119899 Moscow, Russia

Abstract. *Chlamydomonas* has two photobehavioral responses, phototaxis and photoshock. Rhodopsin is the photoreceptor for these responses and the signal transduction process involves transmembrane Ca^{2+} fluxes. This causes transient changes in flagellar beating, ultimately resulting in phototaxis or photoshock. To identify components that make up this signal transduction pathway, we generated nonphototactic strains by insertional mutagenesis. Seven new phototaxis genes were identified (*ptx*2 - *ptx*8); alleles of six of these are tagged by the transforming DNA and therefore should be easily cloned. To order the mutants in the pathway, we characterized them electrophysiologically, behaviorally, and structurally. *ptx*5, *ptx*6, and *ptx*7 have normal light-induced photoreceptor currents (PRC) and flagellar currents (FC) but their pattern of swimming does not change in the normal manner when the intraflagellar Ca^{2+} concentration is decreased, suggesting that they have defects in the ability of their axonemes to respond to changes in Ca^{2+} concentration. *ptx*2 and *ptx*8 lack the FC but have normal PRCs, suggesting that they are defective in the flagellar Ca^{2+} channel or some factor that regulates it. *ptx*4 mutants have multiple eyespots. *ptx*3 mutants are defective in a component essential for phototaxis but bypassed during photoshock; this component appears to be located downstream of the PRC but upstream of the axoneme.

CHLAMYDOMONAS is a motile organism that possesses a primitive "visual" system that allows it to position itself optimally within its environment. Light causes two types of behavioral responses in *Chlamydomonas*. One is phototaxis, which is directed swimming towards or away from a light source. The other, photoshock, occurs when the cell experiences a large change in light intensity. This causes the cell to transiently stop moving and then swim backwards for a short distance, after which it resumes forward swimming in a random direction. For both behavorial responses, the photoreceptor is a rhodopsin-like molecule, and the signal transduction chain involves transmembrane Ca^{2+} fluxes that cause temporary changes in the beating of the two flagella (for reviews see Sineshchekov, 1991; Witman, 1993 and Fig. 1).

The *Chlamydomonas* photoreceptor is located peripherally near the cell's equator in a complex structure called the eyespot. The eyespot is composed of two or more layers of carotenoid granules covered by the chloroplast envelope and the plasma membrane (Melkonian and Robenek, 1984; Witman, 1993). The photoreceptor molecule is believed to be located in the plasma membrane (or possibly in the chloroplast envelope) immediately over the granules (Melkonian and Robenek, 1984). The granules make the photoreceptor unidirectional by shielding it from light passing through the cell body, and by reflecting light that has fallen directly on the eyespot, and then passed through the photoreceptor back onto the photoreceptor membrane (Foster and Smyth, 1980). This results in an approximately eightfold modulation of the amount of light reaching the photoreceptor membrane (Harz et al., 1992), giving the cell the cues it needs to orient to light. The rhodopsin-like photoreceptor protein (Foster et al., 1984) uses, as a cofactor, all-*trans* retinal which is isomerized to 13-*cis* retinal during photostimulation (Hegemann et al., 1991; Lawson et al., 1991).

Extracellular recordings of single cells of the green alga *Haematococcus* (Litvin et al., 1978) revealed that a flash of light produces two major currents. Similar extracellular recordings of single cells (Harz and Hegemann, 1991) and populations of *Chlamydomonas* (Sineshchekov et al., 1992) revealed the same cascade of electrical responses. The first, which appears within 0.5 ms of the flash, originates in the eyespot and is called the photoreceptor current (PRC).[1] Removal of Ca^{2+} from the extracellular medium decreases this current by 70%, suggesting that at least part of the signal is due to Ca^{2+} influx. The amplitude of the

Please address all correspondence to Dr. G. B. Witman, Worcester Foundation for Biomedical Research, 222 Maple Avenue, Shrewsbury, MA 01545. Tel.: (508) 842-8921. Fax: (508) 842-3915.

1. *Abbreviations used in this paper*: FC, flagellar current; PRC, photoreceptor current.

© The Rockefeller University Press, 0021-9525/95/10/427/14 $2.00

PRC is dependent on the intensity of the stimulus. If the PRC is large enough, it triggers a second current that originates within the flagella. The flagellar current (FC) is an all-or-none response; once triggered, its amplitude is independent of the intensity of the light stimulus. The FC is carried entirely by Ca^{2+}.

It is hypothesized that the PRC and FC alter the intraflagellar Ca^{2+} concentration which in turn controls the beating of the two flagella. The two flagella of *Chlamydomonas* respond differentially to submicromolar levels of Ca^{2+}. When demembranated cell models were reactivated in nominal 10^{-8} M Ca^{2+}, both axonemes beat and the models swam much like living cells. However, if Ca^{2+} was decreased slightly, the *trans*-axoneme (the one farther from the eyespot) was inactivated. In contrast, a slight increase in Ca^{2+} caused the *cis*-axoneme to be inactivated (Kamiya and Witman, 1984). Increasing Ca^{2+} concentration at least two orders of magnitude caused the waveform of isolated axonemes to change from that seen in forward swimming to the waveform seen when cells swim backwards during photoshock (Bessen et al., 1980). Thus, it has been proposed that light striking the photoreceptor leads to a temporary change in the Ca^{2+} concentration within the flagella. This affects the axonemes and results in the turning responses needed for phototaxis, or the change in waveform needed for photoshock.

While much is known about the general pathway, very little is known about its specific components. A few genes involved in this pathway have been identified. These include: *ptx*1, thought to encode an axonemal component (Horst and Witman, 1993); *agg*1, believed to be involved in the control of phototactic sign (Smyth and Ebersold, 1985); *ey*1, which affects eyespot structure (Hartshorne, 1953); and the genes *lts*1 and *car*1, needed for production of the retinal cofactor (Iroshnikova et al., 1982; Foster et al., 1984). As a first step in the identification and characterization of other components of this pathway, we have undertaken a mutant screen to identify additional genes that are required for phototaxis. It is expected that these genes will encode photoreceptors and channels that are required for direct transmission of information, low and high Ca^{2+} sensors in the axoneme, kinases, phosphatases and other factors that modulate the pathway, as well as polypeptides needed for sorting and localizing the signal transduction apparatus to the proper place in the cell. As the sensory cells of vertebrate visual and olfactory systems are modified cilia, and have retained many of the signaling elements of the motile cilia from which they were derived evolutionarily (Witman, 1990), the information learned from studies on *Chlamydomonas* phototransduction should further our understanding of these homologous events in higher organisms.

In this study, we used insertional mutagenesis to identify seven new genes that encode components of the pathway. We have used behavorial and electrophysiological analyses to order the mutations along the pathway. Three of the mutations affect only phototaxis and are likely to involve defects in axonemal proteins. Two other mutations affect both phototaxis and photoshock, and appear to involve the activity of Ca^{2+} channels in the flagellar membrane. These mutations provide evidence that phototaxis and photoshock use common elements. Yet another mutation results in multiple, misplaced eyespots in otherwise normal cells. The seventh mutant appears to have a defect

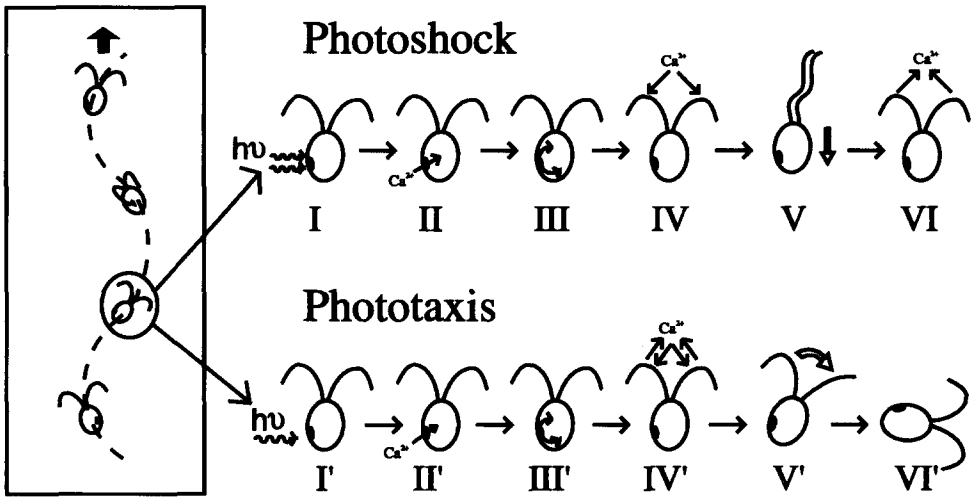

Figure 1. Chlamydomonas photoresponses. (*Inset*) As the cell swims forward, it rolls around its longitudinal axis, so that the eyespot scans the environment through a full 360° approximately twice each second. *Photoshock* (*upper row*): (I) Light activates a rhodopsin-like photoreceptor in the eyespot. (II) This triggers an influx of Ca^{2+} into the cell body. (III) The influx of Ca^{2+} causes a depolarization which spreads throughout the cell (*arrows*). (IV) If the depolarization is great enough, voltage-gated Ca^{2+} channels located in the flagellar membrane are opened and Ca^{2+} flows into the flagella, greatly raising the intraflagellar Ca^{2+} concentration. (V) The elevation in Ca^{2+} is detected by axonemal proteins and causes changes in the flagellar waveform, resulting in photoshock. (VI) After a short period of time, Ca^{2+} is returned to the basal level by the action of Ca^{2+} pumps and the cell returns to normal forward swimming. *Phototaxis* (*lower row*): Phototaxis results when a weaker stimulus is received. Steps I′ and II′ are the same as in photoshock; however, the depolarization (III′) resulting from the weaker stimulus is inadequate to induce the all-or-nothing flagellar current. (IV′) The depolarization nevertheless induces small changes in intraflagellar Ca^{2+}. This could be accomplished if there is a continuous basal current in the flagellum that is the result of Ca^{2+} entering through the voltage-gated Ca^{2+} channel and exiting through the action of Ca^{2+} pumps. If the change in membrane potential altered the activity of either the channels or the pumps, the intraflagellar Ca^{2+} concentration would be raised or lowered slightly. Alternatively, there could be a second flagellar Ca^{2+} channel sensitive to low voltage that allows only small amounts of Ca^{2+} to enter. (V′) This change in Ca^{2+} is detected by low Ca^{2+} sensors in the axoneme, ultimately leading to brief changes in the beating of the *cis*- or *trans*-flagellum to cause phototactic steering. (VI′) After the turn, the cell returns to straight swimming in a direction parallel to the stimulus beam.

downstream of the photoreceptor channel but upstream of the axoneme. For six of these genes, we have identified alleles that were generated by the integration of exogenous DNA; this should make it relatively straightforward to clone the "tagged" genes that correspond to these mutations. These studies demonstrate the promise of this system for genetic and molecular genetic analysis of a cilium-based eukaryotic phototransduction pathway.

Materials and Methods

Strains

g1 (*nit*1, *agg*1, *mt*+) was derived from a cross of *nit*1-305 (from J. Rosenbaum) to CC124 (Chlamydomonas Genetics Stock Center Department of Botany, Duke University, Durham, NC). This strain shows strong negative phototaxis and is easily transformed.

B214 (*nit*1, *ac*17, *agg*1, *mt*−) was made by three backcrosses of g1 to *ac*17 *mt*− strains. The first cross was g1 to CC530 (*ac*17, *nit*1, *nit*2, *mt*−) (Chlamydomonas Genectics Stock Center). The second and third crosses were g1 to an *ac*17 *mt*− offspring of the first and second cross, respectively.

B207 (*ptx*1-1, *nit*1, *mt*+) was made by four backcrosses of g1 to *ptx*1-1 *mt*− strains. The first cross was g1 to h41(3/3) (from C. Horst). The next three crosses were g1 to a *ptx*1-1, *mt*− offspring of the previous cross. B207 is here referred to as *ptx*1-1.

Growth Medium

Chlamydomonas was grown in Sager and Granick (1953) medium I altered to have 0.0022 M KH_2PO_4 and 0.00171 M K_2HPO_4 (here referred to as M medium), M medium plus 0.0075 M sodium acetate (here referred to as R medium), or Sager and Granick (1953) medium II modified to have 0.003 M KNO_3 as the nitrogen source (here referred to as SGII-NO_3 medium).

Transformation

DNA used for transformation was either pMN24 (Fernandez et al., 1989) or pGP505, both of which contain the *NIT*1 gene as a selectable marker. pGP505 is a smaller derivative of pMN24. It contains the 9-kb XbaI to EcoRI fragment of pMN24 and a 0.2 kb EcoR1 fragment carrying the *E. coli supF* gene (Seed, 1983) added to facilitate the cloning of mutant genes. Transformation was carried out by the glass bead method of Kindle (1990). After removing the cell walls with gametic autolysin, $\sim 10^7$ cells were vortexed in 5% polyethylene glycol 8000 (Sigma Chem. Co., St. Louis, MO) (0.4 ml total) with 0.3 g of glass beads and plasmid DNA. Cells were vortexed twice, first for 15 s, followed by an additional 10 s, 2.5 min later. The cells were washed and plated on SGII-NO_3 medium. After about one week, colonies appeared and were picked into liquid medium and assayed for phototaxis.

Two mutagenesis experiments were carried out. In the first experiment 3 μg of supercoiled pMN24 was used. 5551 individual transformants were examined and 64 were found with phototaxis defects. However, linkage between the *ptx* mutation and integrated DNA was found in only four out of 25 randomly chosen lines. In the second experiment 1 μg of linear pGP505 was used. 2978 lines were screened and 12 were found with phototaxis defects. Of these, three lines could not be mated. Linkage was found in eight of the remaining lines.

Phototaxis Assays

Photoaccumulation. For rapid screening of phototaxis mutants, cells were grown in 5 ml of medium in 13 × 100-mm glass tubes until light green. The tubes were placed ~60 cm in front of a 200-W halogen lamp and irradiated for 2–5 min. Wild-type cells swim to the back side of the tube and band in a tight vertical line on the glass. Transformants which did not exhibit this phototactic behavior were readily identified and subjected to a more rigorous phototaxis assay.

Photo-orientation. Phototactic ability was measured by quantifying the behaviors of the mutants at various light intensities and comparing to the behavior of wild-type cells under identical conditions. The apparatus for observing phototaxis is described in Moss et al. (1995). It consists of a 0.8-mm deep chamber constructed of two coverslips and has fiber optic cables coming in from two sides to deliver the actinic beam. Cells are observed under nonactinic dim red light with a CCD camera mounted on a Zeiss Universal microscope. The actinic beam (488 nm) is produced by a 10-mW argon laser with the intensity controlled by neutral density filters. An ExpertVision Motion Analysis system (Motion Analysis Corp., Santa Rosa, CA) was used to collect the video data for 15 s (at a rate of 15 frames per second) starting 10 s after the actinic beam was turned on. The images were digitized and two-dimensional traces of the cells' paths calculated by ExpertVision. These traces were analyzed with either the direction of travel [dir(t)] operator of the ExpertVision Motion Analysis system, or self-developed software (available on request) that calculates mean angles of paths using the circular statistical methods of Batschelet (1981).

To examine the distribution of swimming directions, software was developed that calculates the mean angles (Batschelet, 1981) of the paths and plots the distribution on a polar histogram (see Moss et al., 1995 for details on the calculation and software). A mean angle is the average direction (sampled at 15 Hz) taken by a cell as it travels through the viewing field. When these are plotted on a polar histogram, the bars show the direction traveled and the percent of cells that traveled in that direction. A nonphototactic population will show an even distribution over the entire 360°. Cells showing negative taxis will have a biased distribution of mean angles centered around 180° when the light is incident at 0°, whereas the distribution will be centered around 0° for positively phototactic cells. The tightness of this distribution is related to the strength of taxis.

Although the distribution of mean angles is very useful for displaying the behavior of a population of cells, it does not readily yield a single parameter that is convenient for comparing mutants at many light levels. To obtain such a parameter, cosine of the dir(t) operator was calculated. The dir(t) operator calculates the angle traveled by the cells as they move through the viewing field. The cos(dir(t)) of a cell traveling directly towards the actinic beam would be +1 whereas that of a cell traveling directly away would be −1. Averaging the cos(dir(t))s of all the cells in a population gives a numerical value for phototaxis (Zacks et al., 1993). A random swimming population would have a mean cosine of 0; for phototactic populations the mean cosines range from >0 to 1 (positive phototaxis) and <0 to −1 (negative phototaxis). The strength of phototaxis is directly related to the absolute value of the mean cosine. A mean cosine of 0 also can be obtained if the population contains equal numbers of positively and negatively phototactic cells, but this situation can be distinguished from that in which the cells are swimming in random directions because it results in a bias in the distribution of swimming angles about 0 and 180° in the polar histograms.

Photoshock Assay

Photoshock was assayed by monitoring the swimming speed of a population of cells in response to a flash of light (Hegemann and Bruck, 1989) administered through the epi-illumination port. Cells were monitored by videomicroscopy with dim red illumination. ExpertVision motion analysis was used to analyze the paths taken by the cells and to calculate the mean speed of the population at 33-ms intervals. A flash of light causes wild-type cells to stop swimming briefly and then swim backwards for 0.1–0.5 s, after which the cell resumes forward swimming. This can be seen in the plots as a sharp drop in speed caused by the stop and backwards swimming, followed by a resumption of normal speed as the cells return to forward swimming.

Depletion of Calcium In Vivo

Cells were washed once and resuspended in an equal volume of 0.5 mM EGTA in growth medium M without divalent cations (1.7 mM Na citrate, 0.37 mM $FeCl_3$, 3.7 mM NH_4NO_3, 2.2 mM KH_2PO_4, 1.71 mM K_2PO_4, 0.5 mM EGTA). In the absence of added Ca^{2+}, this concentration of EGTA should be adequate to ensure that free Ca^{2+} in the medium remains at or below 10^{-9} M. Swimming behavior was observed by dark field light microscopy 15 min after initial suspension in EGTA-containing medium.

Analysis of Swimming Speed

ExpertVision Motion Analysis was used to analyze the paths taken by the cells and calculate the mean speed of the population. Data was collected for 15 s starting 10 s after the actinic beam was turned on.

Electrophysiology

Photoinduced currents were measured by the population method of Sineshchekov et al. (1992). A cell suspension (2×10^6 cells/ml) was placed in a rectangular cuvette ($2 \times 60 \times 25$ mm) and excited by a flash from one side at a 45° angle. The electrical current was measured in a vertical plane and amplified with an Axopatch amplifier (Axon Instruments, Foster City, CA). pCLAMP 5.5 (Axon Instruments) was used for data acquisition and analysis.

Cells to be analyzed were grown in liquid M medium bubbled with 5% CO_2. Cells were spun down, resuspended in measuring medium (1.5 mM Hepes, 0.1 mM BAPTA, 0.2 mM $CaCl_2$, 1.75 mM KOH; final pH = 6.8) and allowed to adapt to this medium for 1–3 h before analysis. Wild-type cells were strongly phototactic in this medium.

Genetic Analysis

The techniques used for mating and tetrad analysis were as described by Levine and Ebersold (1960) and Harris (1989). Zygotes were hatched on solid R medium and dissected using a glass needle held by a Newport micromanipulator (1-axis, 36S Tilt Platform). The meiotic progeny were allowed to grow for 3–5 d, and then transferred to 5 ml of liquid R medium. After an additional 5–7 d, the progeny were scored for photo-orientation as described above. Progeny that swam away from the light were scored as *PTX* while those that swam in random directions were scored as *ptx*. *NIT*1 was scored by spotting 5 μl of cells onto SGII-NO_3 solid medium; *NIT*1 cells grew while *nit*1 cells bleached and died.

Other Procedures

DNA was isolated by digesting ~0.3 ml of packed cells with 0.5 ml of Proteinase K (1 mg/ml) in 5% Na lauryl sulfate, 20 mM EDTA and 20 mM Tris, pH 7.5 at 50°C for 12–16 h. Na acetate was added to 1.5 M, the mixture extracted once with 50% phenol/50% chloroform, once with chloroform, and the DNA then precipitated with ethanol. DNA was resuspended in TE and a portion digested with PstI. Gel electrophoresis and Southern blotting were performed according to standard procedures (Sambrook et al., 1987).

Electron microscopy was carried out using the fixation and embedding procedure of Hoops and Witman (1983).

Results

Identification of Seven New Genes Required for Phototaxis

Phototactic mutants were generated by insertional mutagenesis. Transformation in *Chlamydomonas* occurs primarily through nonhomologous recombination, making foreign DNA an effective mutagen (Tam and Lefebvre, 1993). In addition, the inserted DNA can be used as a "tag" to clone the mutated gene. Individual transformants were first screened to find ones that failed to photoaccumulate. Failure to photoaccumulate can be due to a defect in either phototaxis or motility. To separate these classes, the response of individual cells to photostimulation was examined microscopically, and only those lines with phototactic defects, but no grass motility defects (see Motility below) were selected for further analysis.

Mutants found to be defective in phototaxis were crossed to wild type and the progeny examined to determine if the mutations were linked to the inserted DNA. Twelve *ptx* mutations resulting from the insertion of exogenous DNA were identified (see below). Recombination analysis of these twelve tagged mutations and two additional untagged mutations showed that the collection represents at least seven new genes (Table I). No alleles of the previously identified gene, *ptx*1, were obtained. The number of

Table I. Genetic Analysis of ptx Mutants

	*ptx*1-1	*ptx*2-1	*ptx*3-1	*ptx*3-2	*ptx*3-3	*ptx*3-4	*ptx*4-1	*ptx*4-2	*ptx*5-1	*ptx*5-2	*ptx*5-3	*ptx*6-1	*ptx*6-2	*ptx*7-1
*ptx*1-1														
*ptx*2-1	0:0:1													
*ptx*3-1		6:0:7												
*ptx*3-2	2:0:2	1:2:11												
*ptx*3-3			24:0:0											
*ptx*3-4			60:0:0	26:0:0	22:0:0									
*ptx*4-1	0:0:2	0:0:1	1:1:6	1:0:5										
*ptx*4-2		3:0:0					23:0:0							
*ptx*5-1				0:2:8										
*ptx*5-2	2:2:7	0:1:0		0:0:2		3:3:10	0:0:3		46:0:0					
*ptx*5-3				0:0:2					21:0:0					
*ptx*6-1	8:0:3	1:0:1		0:1:8		2:3:6	0:1:1	0:0:1	1:0:11	0:5:9	1:0:2			
*ptx*6-2				0:2:4					2:1:7	2:1:3	1:0:1	21:0:0		
*ptx*7-1	4:1:8	3:1:1		1:0:4		6:4:6	0:0:1	1:0:1	2:6:2	6:1:3	1:1:0	0:2:9	1:0:4	
*ptx*8-1	0:0:2	5:1:25		0:0:3			1:0:1			2:2:4		0:0:2		1:1:1

Cells carrying *ptx* mutations were mated to each other, tetrads dissected, and the offspring scored for the ability to photo-orient. Numbers shown above are the ratio of parental ditypes:nonparental ditypes:tetratypes. Identification of one or more recombinant progeny (from a nonparental ditype or tetratype) was taken as evidence that the mutations are in different genes. If no recombinants were found in 20 or more tetrads then the mutations were considered to be allelic. Not every pair-wise cross was made; when it was determined that two mutations were allelic, further crosses were made with only one of the two.

alleles identified ranged from one each of *ptx*2, *ptx*7, and *ptx*8 to four alleles of *ptx*3.

Linkage between the Inserted DNA and the Phototaxis Defect

Mutant alleles generated by insertional mutagenesis are valuable because they can provide a straightforward way to clone the affected genes. However, not all mutants identified after transformation have the defective gene tagged with exogenous DNA (see below). To concentrate effort on the most useful alleles, it is important to identify those which are the result of stable integration of exogenous DNA.

Transformants with phototaxis defects were crossed to wild-type cells and the progeny scored for phototaxis, growth on nitrate (*NIT*1) and for the presence of pUC119 sequences integrated into the genome. pUC119 is the cloning vector in which the nitrate reductase gene was inserted. If the inserted DNA caused the mutation, it will segregate with the phototaxis defect in the offspring and can be used to clone the gene that it has disrupted. Data for a representative allele of each of the genes are shown below.

Crosses of *ptx*2-1 to wild type indicated that *ptx*2-1 was not caused by integration of a functional copy of the nitrate reductase gene (6 PD:2 NPD:17 T). However, Southern analysis showed that the original mutant line contained three independently segregating insertions. One of these insertions segregated with the phototaxis defect (two bands marked with a * in Fig. 2 *A*). The other two segregated independently of the phototaxis defect and each other. The insertion site that contains the functional *NIT*1 is not seen in Fig. 2 *A* because it does not contain any pUC119 sequences.

Linkage was seen between *ptx*3-2 and growth on nitrate

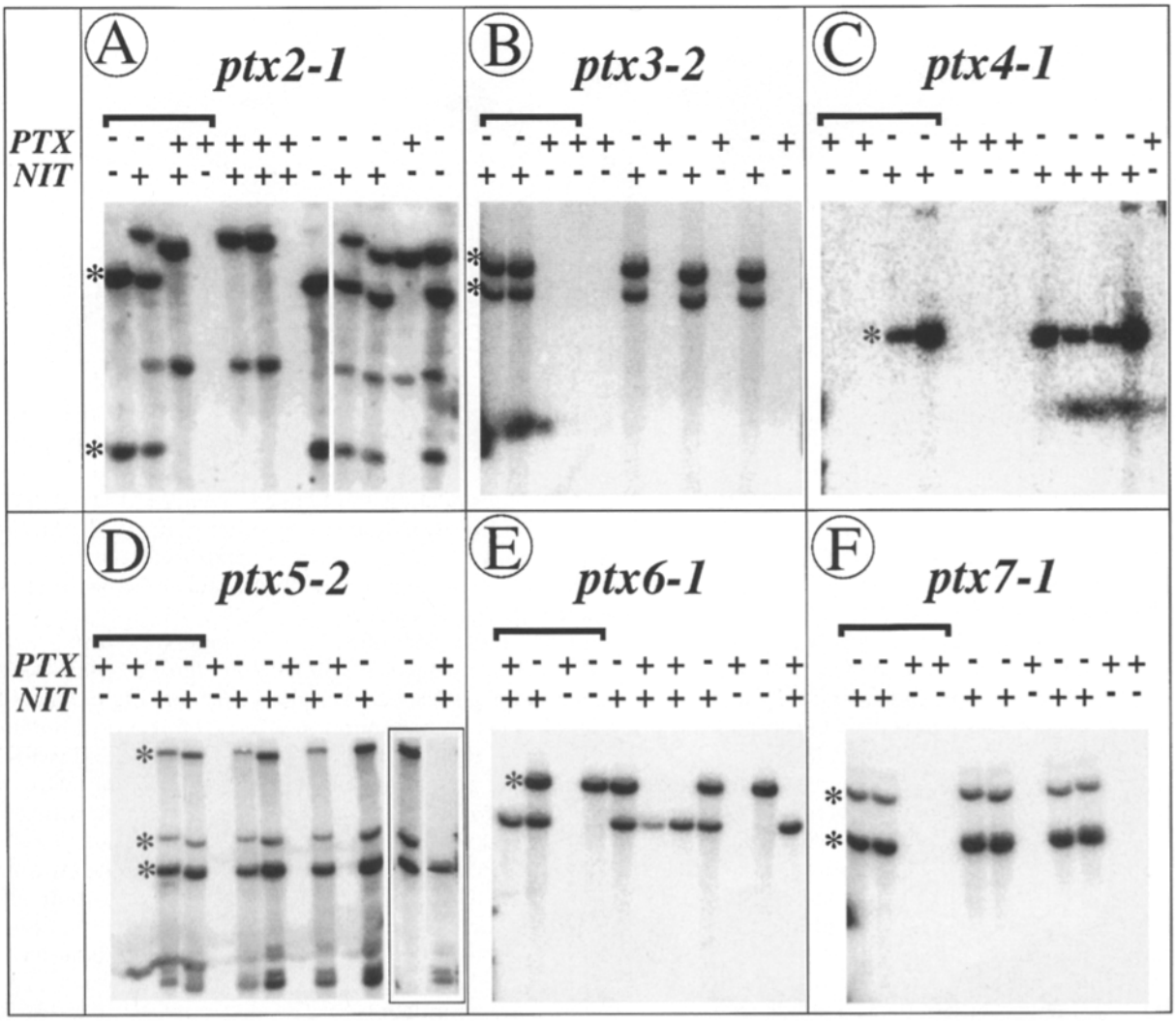

Figure 2. Linkage between inserted DNA and phototaxis defect. Southern blots showing the linkage between the inserted DNA and the phototaxis mutation. Mutant lines were crossed to wild type (B214), tetrads dissected, and the products scored for phototaxis (*PTX*) and the ability to grow on nitrate (*NIT*) as the sole nitrogen source. DNA was isolated from the four products of a single tetrad (marked with a dark bracket) and a single product from 7 to 9 additional tetrads, digested with PstI, separated by agarose gel electrophoresis, transferred to Duralon membrane (Stratagene, La Jolla, CA) and hybridized with radiolabeled pUC119. A phosphorimager was used to collect the data.

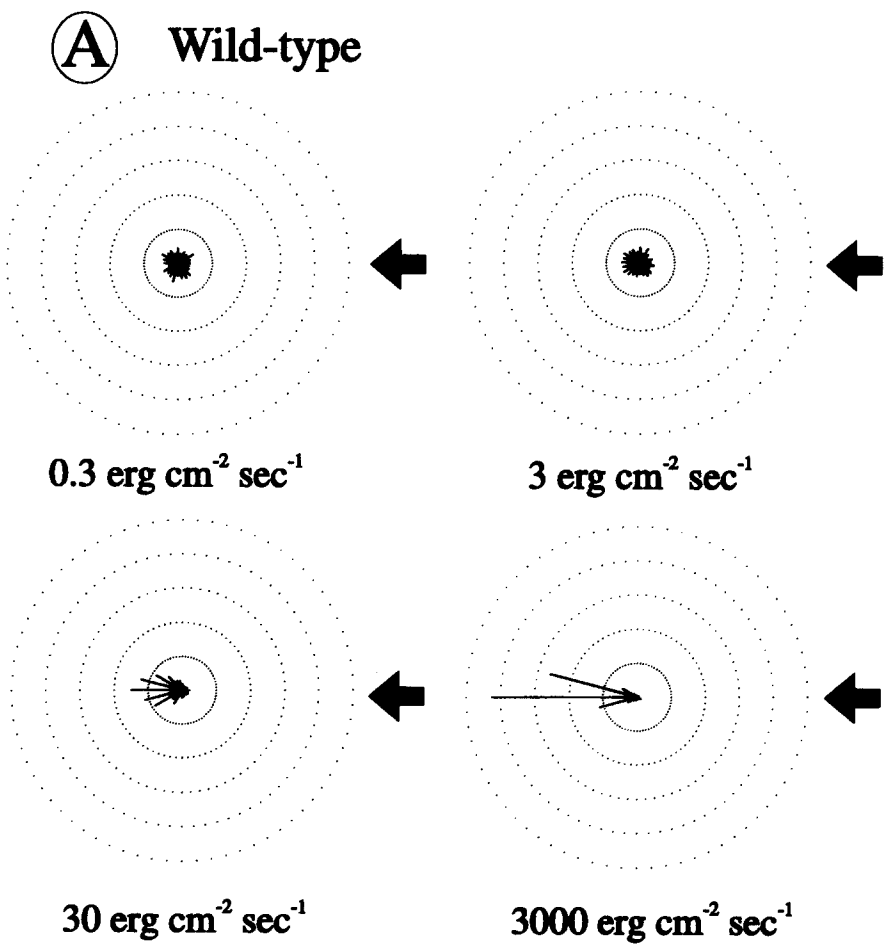

Figure 3. Phototaxis. (*A*) Polar histograms showing the swimming direction of wild-type cells at different intensities of stimulation. The light stimulus was delivered from the right as indicated by the arrows. Each of the 24 bars represents the direction of swimming and the percentage of cells swimming in that direction (15° bin width); each annulus represents 10% of the cells. (*B*) Polar histograms showing the swimming direction of the mutants at a light intensity of 30 erg cm^{-2} sec^{-1} delivered from the right as indicated by the arrows. (*C*) Phototaxis [mean(cos(dir(t)))] is plotted vs intensity of stimulus beam for wild-type and mutant cells. Cells were stimulated with laser light and the cosines of the angles of the paths taken by individual cells were averaged to get a mean cosine for the population. A random swimming population would have a mean cosine of zero, whereas mean cosines range from >0 to 1 (positive phototaxis) and <0 to −1 (negative phototaxis) for phototactic populations. The strength of phototaxis is directly related to the absolute value of the mean cosine.

(29 PD:0 NPD:0 T), indicating that this mutation was caused by integration of a functional copy of *NIT*1. Southern analysis indicated that this strain contained a single insertion that segregated with the nonphototactic phenotype and *NIT*1 (Fig. 2 *B*).

*ptx*4-1 similarly contained a single insertion that segregated with the phototaxis defect and the ability to grow on nitrate (15 PD:0 NPD: 0 T) (Fig. 2 *C*).

*ptx*5 is more complicated. Two tetrads were found in which recombination had occurred between *ptx*5-2 and *NIT*1 (20 PD:0 NPD:2 T). This indicates that the functional copy of *NIT*1 is not causing the phototaxis mutation. When the line was examined by Southern analysis it was found that the mutation was linked to a large array of inserted DNA. In most tetrads, the array segregated as a single unit (Fig. 2 *D*), but in the two tetrads where the nonphototactic phenotype and *NIT*1 segregated apart, the array was split. The bottom set of bands segregated with *NIT*1 while the upper bands segregated with the nonphototactic phenotype (Fig. 2 *D*, *boxed area*).

There was no linkage seen between *ptx*6-1 and *NIT*1 (4 PD:2 NPD:22 T). However, Southern analysis revealed that the line contains two sites of integration, one that segregates with the nonphototactic phenotype (marked with a * in Fig. 2 *E*) and the other with *NIT*1. Therefore, *ptx*6-1 is caused by the insertion of DNA that does not encode a functional nitrate reductase gene.

*ptx*7-1 and growth on nitrate are linked (26 PD:0 NPD:0 T), indicating that *ptx*7-1 is caused by integration of a functional copy of *NIT*1. Southern analysis indicated that this is the only insertion (Fig. 2 *F*).

The *ptx*8-1 mutation is not linked to *NIT*1 (1 PD:0 NPD:1 T), and Southern analysis (using either pUC119 or pMN24 as probes) showed that the phototaxis defect segregated independently of all inserted DNA (data not shown). Thus this mutation is not tagged.

Of the alleles identified in this work, only *ptx*4-2 and *ptx*8-1 are not tagged. It seems likely that these untagged alleles were generated from lines that initially contained multiple sites of integration (e.g., *ptx*2-1). If one of the insertions was unstable and was deleted before cell division, an untagged mutation could arise. Integration of DNA in the *Chlamydomonas* genome is usually associated with deletion of part of the chromosome at the site of integration (Tam and Lefebvre, 1993; Wilkerson et al., 1995; Pazour, G. J., and G. B. Witman, unpublished), making it unlikely that a deletion event would restore a gene at the site of insertion. Alternatively, the untagged mutations could have arisen if a cell containing a spontaneous mutation in a *ptx* gene was transformed. However, this is unlikely because it would require a very high spontaneous mutation frequency, which we have not observed in these cell lines.

Photobehavior

Phototaxis. *Chlamydomonas* can exhibit either positive or

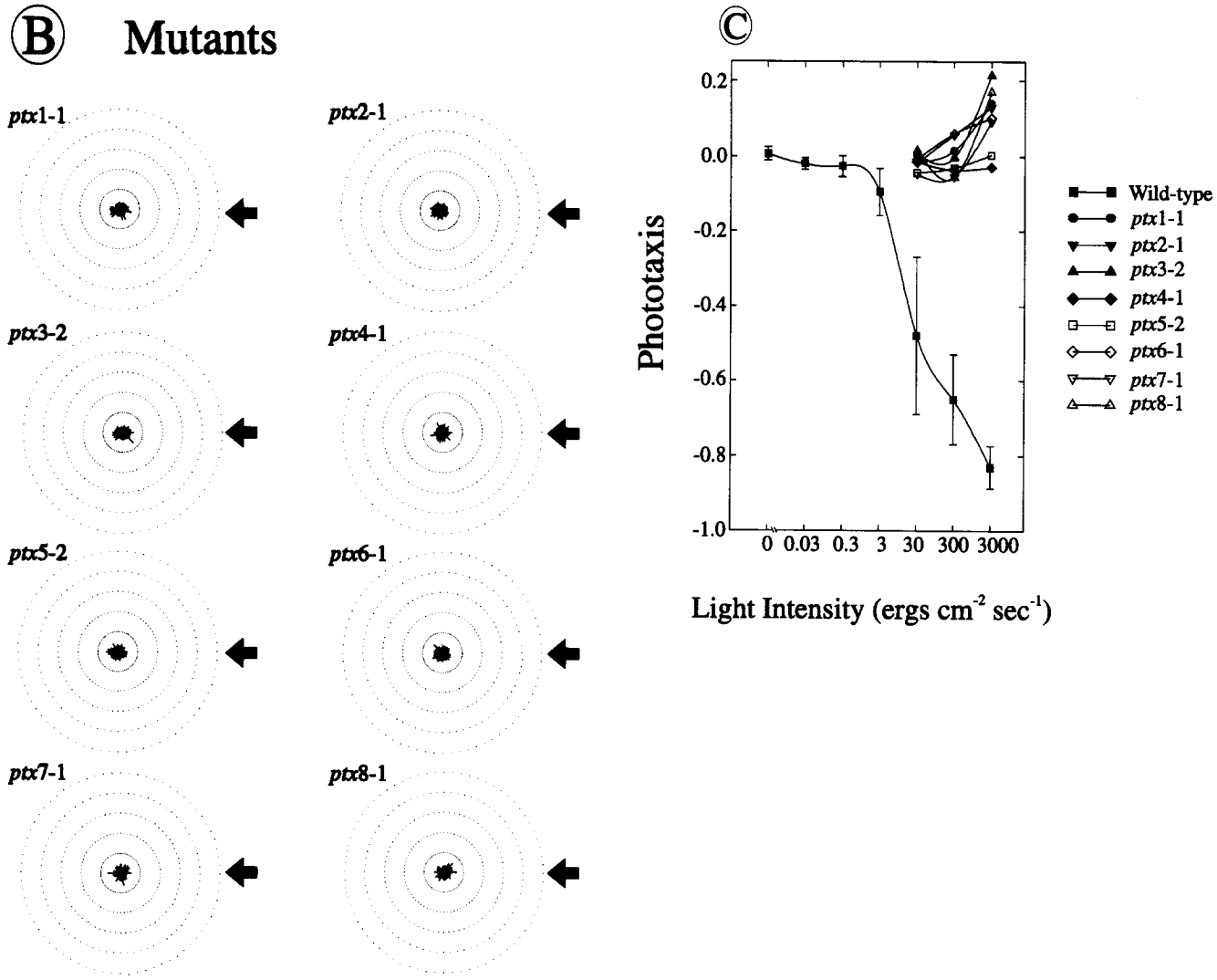

negative phototaxis depending on genotype, growth conditions, and history of light exposure. The *AGG1* gene appears to be the major genetic determinate of phototactic sign (Smyth and Ebersold, 1985). *AGG1* cells show a period of positive taxis that can last for 30 s or more before changing to negative taxis. The natural variant, *agg1* (which is found in the commonly used laboratory strain CC124), causes cells to exhibit strong negative phototaxis (and hence photoaccumulate or "aggregate" under conditions of nonuniform lighting). Under our conditions positive phototaxis is not seen with *agg1* cells, but others (Zacks et al., 1993) have observed a 10-s period of positive phototaxis before the population switches to negative taxis. We used a strain carrying the *agg1* variant as our parental cell line so that we could screen for mutants more easily (by taking advantage of the "aggregation" phenotype) and to minimize the complications caused by the changing of phototactic sign during analysis.

Parental (g1) cells show very little or no bias in orientation until light levels reach 3 erg cm^{-2} sec^{-1} (Fig. 3 *A*), at which point the cells are starting to show a tendency to swim away from the light. This bias becomes stronger as the light intensity increases. At the highest light intensity (3,000 erg cm^{-2} sec^{-1}) almost all cells are swimming away from the light. This trend can be seen when this data is quantitated and plotted (Fig. 3 *C*). The cos(dir(t)) remains very close to zero, indicating random swimming, until the light intensity reaches 3 erg cm^{-2} sec^{-1}. As light intensity increases, the cos(dir(t)) decreases, approaching the theoretical limit of −1 at the highest light level.

A light beam of 30 erg cm^{-2} sec^{-1} induces ~50% of the maximum response in wild-type cells (Fig. 3, *A* and *C*). In contrast, at this same light level no bias is seen in the orientation of any of the mutants (Fig. 3 *B*). The cos(dir(t)) of the mutants is also very near zero at this light level (Fig. 3 *C*). As the light level increases, all of the mutants except *ptx*4-1 and *ptx*5-2 start to exhibit a slight bias in the positive direction (Fig. 3 *C*); *ptx*4-1 and *ptx*5-2 do not show any bias even at the highest light levels. The mechanism causing the slight positive bias in the other mutants is unclear; it could be an artifact caused by a thermal or other beam-induced gradient. In any case, if one assumes that positive taxis of the mutants is equivalent to negative taxis of the parent, then the mutants are at least three orders of magnitude less sensitive than wild-type.

Photoshock. Photoshock was assayed by monitoring the

mean swimming speeds of populations of wild-type or mutant cells during administration of a bright flash of light (Hegemann and Bruck, 1989). In wild-type cells, the flash induces the photoshock response, which in tracings of cell swimming speed vs time is seen as a drastic but brief reduction in the average swimming speed (Fig. 4). *ptx*3-2, *ptx*4-1, *ptx*5-2, *ptx*6-1, and *ptx*7-1 exhibit a photoshock response similar to that of wild-type cells. However, mutants *ptx*2-1 and *ptx*8-1 do not undergo photoshock (Fig. 4), indicating that they are defective in some component necessary for both photoshock and phototaxis. These mutants thus provide evidence that photoshock and phototaxis share a common pathway.

Eyespot Structure

A nonphototactic phenotype could result from either morphological disruption of the eyespot (e.g., as in the *ey* mutations which affect the eyespot's carotenoid layers [Morel-Laurens and Feinleib, 1983; Morel-Laurens and Bird, 1984; Kreimer et al., 1992]), or from mispositioning of the eyespot within the cell. To determine if any of our mutations were affected in these ways, we examined them by both light and electron microscopy.

The eyespot is clearly visible as a bright spot on the side of the cell when viewed by dark-field or epi-illuminated light microscopy. Epi-illuminated light microscopy is particularly good for examining eyespots because it takes advantage of the unique reflective properties of the carotenoid granules to make the eyespots standout from other cell structures. Wild-type cells predominantly have a single eyespot (Fig. 5 *A*), although an occasional cell can be found that contains two eyespots. All of the mutants except *ptx*4-1 and *ptx*4-2 had a single, normal-looking eyespot. *ptx*4-1 and *ptx*4-2 cells had multiple eyespots with some cells having four or more eyespots (Fig. 5 *A*). The position of the eyespots does not appear ordered. The multiple eyespot phenotype segregated with the phototaxis defect (15 tetrads of *ptx*4-1 and 8 tetrads of *ptx*4-2), indicating that the same mutation is causing both the multiple eyespot phenotype and the phototaxis defect. The defect does not appear to be in the segregation of eyespots at cell division, because there are very few cells without eyespots in the population. In addition, flagellar number is normal, suggesting that the presence of multiple eyespots is not simply an accumulation due to an occasional failure of cytokinesis.

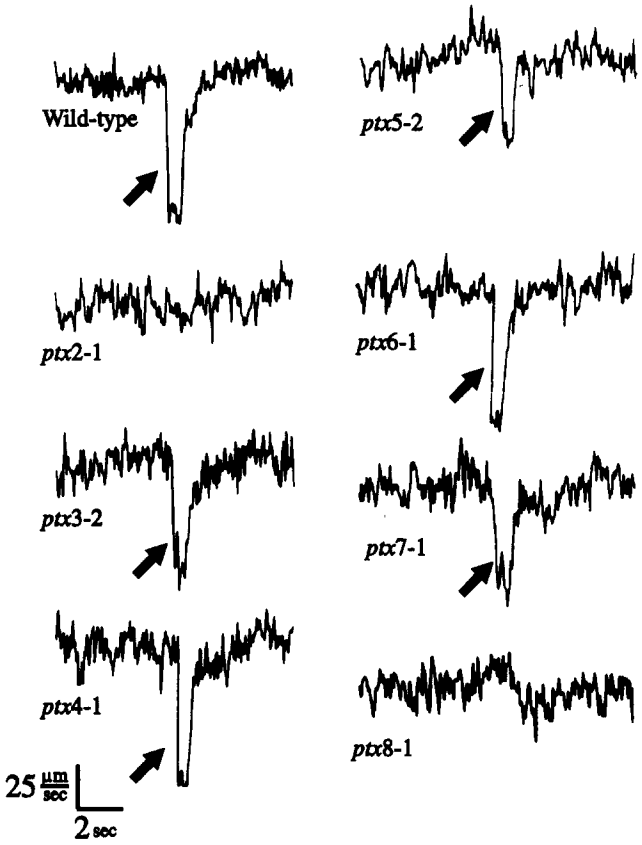

Figure 4. Photoshock was assayed by examining the effect of a flash of light on the swimming speed of a population of cells. The traces show swimming speed as a function of time. If the flash of light causes a photoshock, the speed of the population will drop rapidly but transiently as the cells stop swimming forward, switch to backward swimming, and then resume forward swimming. This is seen in the traces of wild type and several of the mutants as a sharp downward spike (marked with an arrow).

Examination of the eyespot by electron microscopy did not reveal any alterations in eyespot ultrastructure in any of the mutants. Normal carotenoid granules were seen and the thickening of the inner leaflet of the plasma membrane was observed in all of the mutants (data not shown). Cross sections of *ptx*4-1 confirmed that the multiple bright spots seen with light microscopy were indeed eyespots (Fig. 5 *B*).

Electrophysiology

Photostimulation of a *Chlamydomonas* cell produces two major currents. The first occurs in the eyespot. It is an inwardly directed current that is carried largely by Ca^{2+}, and its amplitude is directly related to the intensity of the stimulus. If this current, called the photoreceptor current (PRC), exceeds a threshold level, a second current originating in the flagella is triggered. The flagellar current (FC) is an all-or-none response; its amplitude is constant regardless of the size of the stimulus that triggered it. It is thought to be due to the opening of voltage-gated Ca^{2+} channels, and produces the elevation in intraflagellar Ca^{2+} that causes a photoshock.

These electrical currents were measured by extracellular recording of populations of cells using the technique of Sineschekov et al. (1992). This technique measures the asymmetric currents that occur in a chamber filled with *Chlamydomonas* cells when it is flashed with directional light (Fig. 6 *A*).

A net PRC is generated because of the localization of the photoreceptor and photoreceptor channel in the eyespot. The shielding and reflective properties of the eyespot make cells facing the light eightfold more sensitive to light than those facing away. As a result, cells oriented so that their eyespots are facing the light (cells A and B, Fig. 6 *A*) will produce a larger PRC at a given stimulus than those cells with eyespots facing away from the light (cells C and D, Fig. 6 *A*). The net PRC will be the sum of the large PRCs produced by cells facing the stimulus minus the small PRCs of those facing away.

A net FC is generated because the eyespot is usually lo-

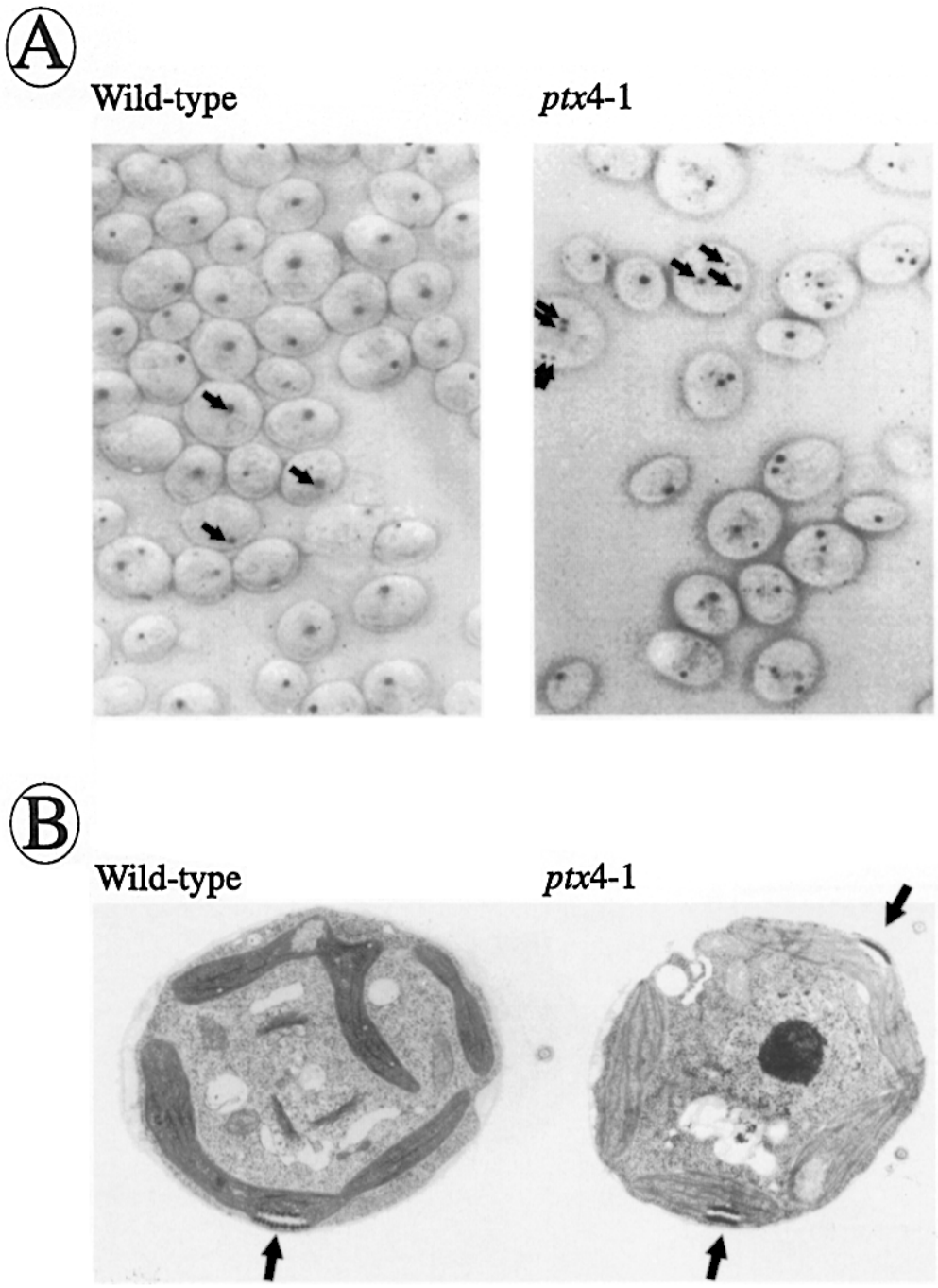

Figure 5. Eyespot structure. (*A*) Eyespots (*arrows*) are visible with epi-illumination because of their reflective properties. Wild-type cells have predominantly one eyespot, whereas most *ptx*4-1 cells have two or more eyespots. (*B*) Electron micrographs of wild-type and *ptx*4-1 cells having one and two eyespots (*arrows*), respectively.

cated slightly rearward of the cell's equator. As a result, cells D and F, and C and E of Fig. 6 *A*, with their flagella facing in the opposite direction from cells A and B, respectively, will have smaller PRCs and thus be less likely to produce FCs that would cancel those produced by cells A and B. This is because in cells C and D the eyespot is on the side of the cell facing away from the light, and in cells E and F the eyespot is oblique to the stimulus beam. Similarly, cells G and H, which are identical to cells B and A except that they have rolled 180° around their longitudinal axes, will have relatively small PRCs and thus be less likely to produce FCs. The resulting net FC will be in the opposite direction from the net PRC (long arrows at top and bottom of Fig. 6 *A*).

Flashing the wild-type strain with light produces a PRC that rises up within 2 ms of the flash and then decays. The PRC is followed by an FC of the opposite sign a few msec later (Fig. 6 *B*).

Mutations in *ptx*2-1 and *ptx*8-1 abolish the FC but do not affect the PRC (Fig. 6 *B*). The lack of the FC suggests that these mutations are in genes that code for components of the flagellar calcium channel, something that regulates the flagellar channel, or something essential for conducting the signal from the eyespot to the flagella. In any case, these results explain why these mutants are unable to undergo the photoshock response (Fig. 4).

As expected, *ptx*1, which is defective in axonemal components (Horst and Witman, 1993), has a normal PRC and

FC. The electrical responses of *ptx*5, *ptx*6, and *ptx*7 also look like wild type (Fig. 6 *B*), suggesting that the defect in each of these mutants also is downstream of Ca^{2+} entry into the flagellum.

Mutations in *ptx*3 alter the amplitude of the PRC (Fig. 6 *B*). Four alleles of this gene have been identified and all have a PRC that is about twofold smaller than wild type.

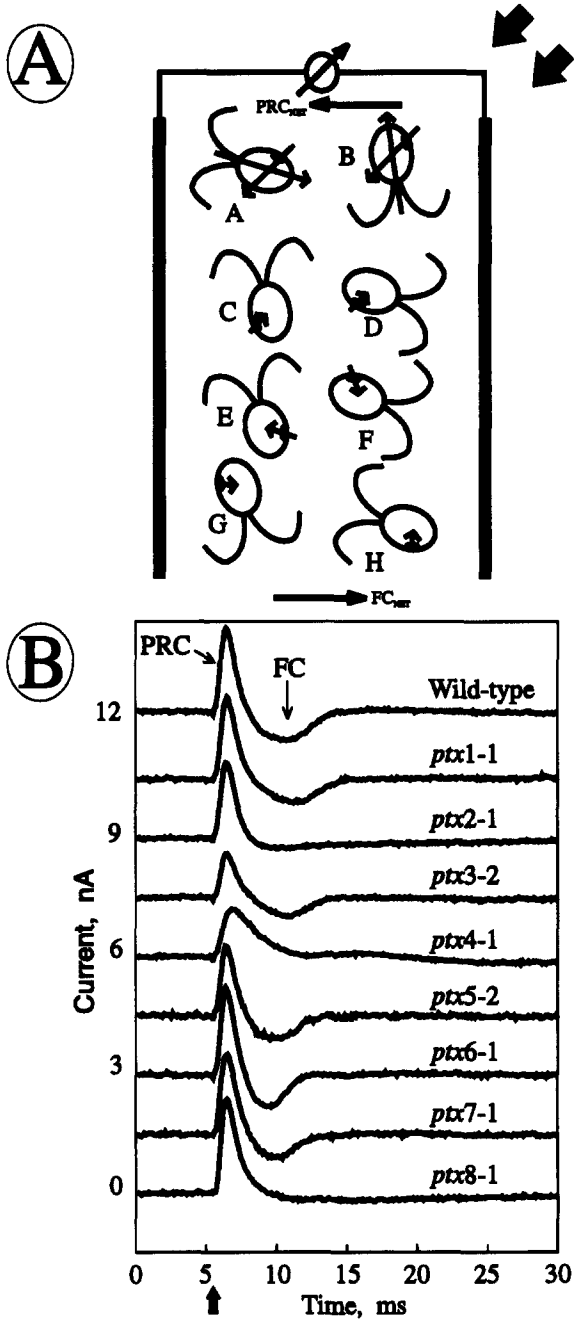

Figure 6. Electrophysiology. (*A*) Schematic representation of the origin of the currents (*thin arrows*) induced by light coming from the upper right (*broad arrows*) and measured by extracellular recording of populations of cells (see text). The relative positions of the electrodes are indicated by the dark vertical bars at the left and right. (*B*) Photoreceptor currents (PRC) and flagellar currents (FC) produced by wild-type and mutant *Chlamydomonas* cells in response to a flash of white light administered at the instant indicated by the filled arrow.

A normal FC is seen because the residual PRC at this light level is above the threshold needed to trigger the FC. This mutant is likely to have a defect downstream of the PRC; the decrease in size of the PRC may be an indirect effect (see Discussion).

The multiple eyespot mutant *ptx*4 has altered photoreceptor and flagellar currents (Fig. 6 *B*). The PRC is slightly broadened while the FC is severely decreased in amplitude, broadened, and changed in sign. It is likely that these changes are due to the presence of multiple eyespots in the cells. This should not have much effect on the net PRC because only eyespots on the side of the cell facing the flash would be stimulated fully. The other eyespots would be analogous to eyespots on wild-type cells facing away from the flash. However, extra eyespots in random positions would be expected to have great effect on the net FC. If the extra eyespots were completely random, no FC would be seen because for every orientation of a cell, another cell would occur in an opposite orientation such that the net FC would equal zero. The presence of a small FC of opposite sign in these cells indicates that the eyespots have a small bias towards the anterior end of the cell.

Flagellar Response to Reduced Ca^{2+}

A differential response of the axonemes to changes in submicromolar levels of intraflagellar Ca^{2+} is believed to form the basis for phototactic steering (Kamiya and Witman, 1984). Demembranated cell models of *Chlamydomonas* swim with normal, relatively straight paths when reactivated in a solution containing $MgATP^{2-}$ and nominal 10^{-8} M Ca^{2+}. When the Ca^{2+} concentration is increased slightly (to 10^{-7} or 10^{-6} M), the *cis*-axoneme is inactivated, causing the cells to turn continuously toward the eyespot. Conversely, when the Ca^{2+} concentration is lowered slightly, the *trans*-axoneme becomes inactivated, and the cells turn continuously away from the eyespot. These in vitro changes are reversible and presumably caused by the same processes which are responsible for the transient changes in flagellar activity during phototactic orientation.

The ability of the *trans*-axoneme to respond to changing intraflagellar Ca^{2+} levels can be tested very simply by resuspending intact cells in a Ca^{2+}-free medium containing EGTA (Kamiya and Witman, 1984). When this is done, the *trans*-flagellum of nearly 80% of wild-type cells becomes inactive within 25 min, causing the cells to swim in circles (Fig. 7 *A*). Under the same conditions, nearly 80% of cells of *ptx*1-1, which have a defect in the ability of their axonemes to respond normally to changes in Ca^{2+} at the submicromolar level (Horst and Witman, 1993), continued to swim straight. When this assay was applied to the new mutants, *ptx*5-2, *ptx*6-1, and *ptx*7-1 all behaved like *ptx*1, indicating that they also are likely to have defects within the axoneme. In contrast, *ptx*2-1, *ptx*3-2, *ptx*4-1, and *ptx*8-1 all behaved like wild type, confirming that they are defective in components of the sensory transduction pathway upstream of the axonemal Ca^{2+} receptors.

Motility

When the swimming behavior of the mutants isolated in this study was examined microscopically, nothing unusual was observed. To quantitatively assess motility, the speed

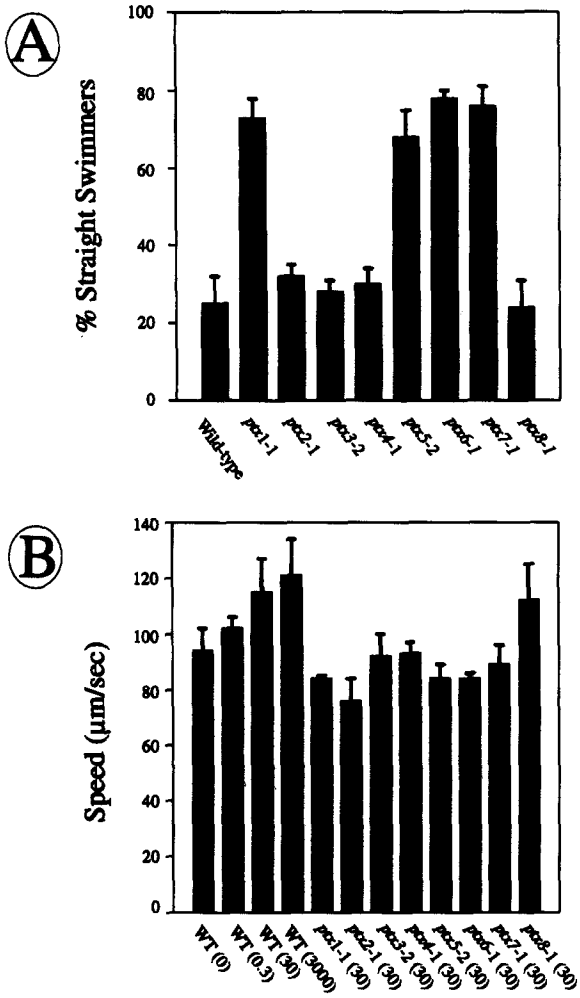

Figure 7. Motility. (*A*) Responses of intact wild-type and mutant cells to reduced Ca^{2+}. Cells were placed in Ca^{2+}-free medium containing 0.5 mM EGTA. This should be adequate to reduce the free Ca^{2+} concentration in the medium to 10^{-9} M or lower. After 15 min, cells were observed by light microscopy and the percent of motile cells that were swimming in straight paths was scored. (*B*) The speed operator of the ExpertVision motion analysis system was used to calculate the swimming speed of populations of wild-type and mutant cells. Cells were treated as during a phototaxis assay. The intensity of the stimulus beam (in erg cm^{-2} sec^{-1}) is shown in parentheses below the sample name.

operator of the ExpertVision motion analysis system was used to analyze mean swimming speed in populations of cells. Speed of wild-type cells increased from 94 μm/s to 121 μm/s as the intensity of the stimulus beam was increased (Fig. 7 *B*). This apparently is due to cells traveling in straighter paths with a smaller helical pitch when phototaxing. The mutants had average swimming speeds ranging from 76 μm/s for *ptx*2-1 to 112 μm/s for *ptx*8-1. Most of these rates are similar to that of wild type in the absence of a stimulus beam; they most likely are slower than wild type at equivalent intensity of the stimulus because the mutants, unlike wild type, do not reduce the pitch of their paths in the presence of a stimulus beam. In any case, none of the mutants appear to have a major defect in their swimming ability.

Discussion

Insertional mutagenesis followed by a mutant screen was carried out to identify components of the *Chlamydomonas* phototransduction pathway. Genetic characterization of 14 new nonphototactic lines identified seven new phototaxis genes, of which six are tagged by the transforming DNA. Behavioral, structural, and electrophysiological characterization were used to order the mutations along the phototransduction pathway (Table II and Fig. 8), where they fell into four phenotypic classes.

The first class, consisting of *ptx*2 and *ptx*8, has defects in phototaxis and photoshock. These mutants have a normal PRC but are missing the flagellar calcium current, indicating that they are downstream of the PR channel and upstream of Ca^{2+} entry into the flagellum. These mutants reveal that common components are essential for generating the small Ca^{2+} fluxes responsible for phototaxis and the larger Ca^{2+} influx responsible for photoshock. The mutants also indicate that flagellar channel activity is involved in phototaxis as well as photoshock.

One possibility is that a single voltage-sensitive Ca^{2+} channel is responsible for both behaviors (Fig. 8 and see Witman, 1993). This channel would open in an "all-or-nothing" manner in response to a large depolarization and thus result in the massive increase in intraflagellar Ca^{2+} which induces photoshock. The same channel also would be involved in the generation of a small continuous basal current which is modulated in response to small voltage fluctuations to generate the submicromolar changes in Ca^{2+} needed for phototaxis. A defect in this channel, or in a protein necessary for expression or functioning of the channel, would therefore affect both phototaxis and photoshock.

Alternatively, the flagellar membrane could contain two types of Ca^{2+} channels. The first type would be a low conductance Ca^{2+} channel which exhibits a graded response with increasing voltage and allows only relatively small amounts of Ca^{2+} to enter the flagellum. In response to small depolarizations, this channel would mediate the entry of submicromolar amounts of Ca^{2+} and phototactic steering. The second type of channel would be a high conductance, Ca^{2+}-activated Ca^{2+} channel. When intraflagellar Ca^{2+} reached a certain threshold due to the action of the first channel, this second channel would be activated, leading to the large Ca^{2+} influxes necessary for photoshock. A defect which affected the functioning of the low conductance Ca^{2+} channel would therefore eliminate both phototaxis and photoshock.

Mutants analogous to *ptx*2 and *ptx*8 have been isolated in *Paramecium*; these are called *pawn* or *cnr* mutants and lack the ability to swim backwards (Kung, 1971; Takahashi, 1979). They are missing a Ca^{2+}-channel activity that is located in the cilia. The gene product of *cnr*C has been purified more than 500-fold using a bioassay. It appears to be a soluble $<\sim$30-kD protein that is required for activity of the ciliary Ca^{2+} channel (Haga et al., 1984); however, nothing more is known about the protein.

The second phenotypic class consists of *ptx*5, *ptx*6, *ptx*7, and the previously identified *ptx*1. These have normal electrical responses but behave aberrantly in EGTA, suggesting that they have defects in components of the trans-

*Table II. Summary of ptx mutant phenotypes**

Gene	Tagged alleles	Phototaxis	Photoshock	Eyespot	Photoreceptor current	Flagellar current	Behavior in low Ca^{2+}	Motility	Proposed defect
ptx1	No	−	+	+	+	+	−	+	Axonemal Response to Ca^{2+}
ptx2	Yes	−	−	+	+	−	+	+	Voltage-dependent Ca^{2+} channels not activated
ptx3	Yes	−	+	+	+‡	+	+	+	Abnormal resting potential
ptx4	Yes	−	+	−§	−	−	+	+	Maintenance of eyespot number
ptx5	Yes	−	+	+	+	+	−	+	Axonemal response to Ca^{2+}
ptx6	Yes	−	+	+	+	+	−	+	Axonemal response to Ca^{2+}
ptx7	Yes	−	+	+	+	+	−	+	Axonemal response to Ca^{2+}
ptx8	No	−	−	+	+	−	+	+	Voltage-dependent Ca^{2+} channels not activated

*+, normal; −, mutant.
‡Photoreceptor current slightly smaller than normal (see Discussion).
§Has multiple eyespots.

duction pathway that are located after the point at which Ca^{2+} concentration is altered in the flagella. Indeed, *ptx1* previously was shown to be deficient in two ~75-kD axonemal proteins (Horst and Witman, 1993); it is likely that the other mutants also have defects in genes encoding axonemal proteins. These could include proteins that sense the changes in submicromolar levels of Ca^{2+}. The Ca^{2+}-binding proteins calmodulin and centrin/caltractin are present in *Chlamydomonas* flagella (Gitelman and Witman, 1980; Huang et al., 1988; LeDizet and Piperno, 1995). However, it is not likely that *ptx5*, *ptx6*, or *ptx7* are calmodulin mutations, because the alleles that we identified probably are null, and calmodulin, which is encoded by a single gene in *Chlamydomonas* (Zimmer et al., 1988), undoubtedly is essential in this organism as it is in *Saccharomyces cerevisiae* (Davis et al., 1986) and *Schizosaccharomyces pombe* (Takeda and Yamamoto, 1987). It also is not likely that any of these are centrin mutants because *vfl2*, which is a point mutation of centrin (Taillon et al., 1992), causes abnormal motility (Kuchka and Jarvik, 1982), whereas these *ptx* mutants have normal motility. Therefore, further analysis of this class of mutations may reveal new Ca^{2+}-binding regulatory proteins. On the other hand, these mutants could be defective in proteins required for the transport of specific polypeptides into the flagella, in proteins such as kinases that might transmit the signal from the Ca^{2+} sensor to the next element in the pathway, in components such as the central microtubules, radial spokes or dynein regulatory complex that control dynein arm activity, or possibly in subunits of an axonemal dynein itself. Ultimately, the temporary inactivation of one flagellum or the other in response to Ca^{2+} is likely to involve regulation of the dynein arms (Fig. 8).

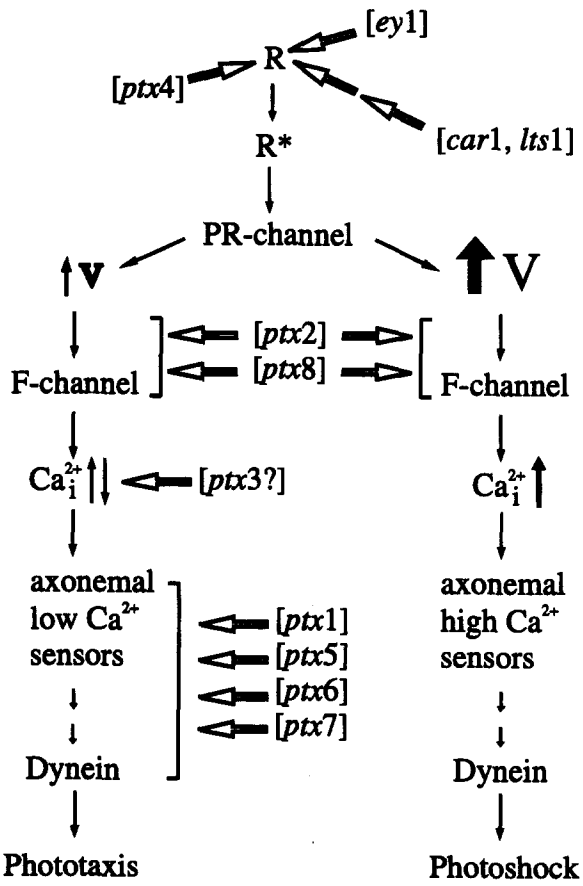

Figure 8. The phototransduction pathway. Schematic of the *Chlamydomonas* phototransduction pathway showing the proposed location of the defects in the *ptx* mutants, as well as the previously described *ey1*, *car1*, and *lts1* mutants (see text). The pathway begins with rhodopsin (*R*, *R**) in the eyespot, goes through a photoreceptor channel (*PR-channel*) which causes depolarization (↑*V*) of the cell, and then branches, with one branch going to phototaxis and the other to photoshock.

The mutations in this class are analogous to the *atalantas* mutants of *Paramecium*. These mutants are impaired in their ability to swim backwards when stimulated by heat or ions. They have normal membrane properties including the inward Ca^{2+} current that is defective in *pawns* and *cnrs*. The *atalantas* mutants, in contrast to wild type, do not swim backwards when the membrane is disrupted and Ca^{2+} is allowed in (Hinrichsen et al., 1984).

The third class, represented by *ptx3*, is at least three orders of magnitude less phototactic than wild type, but has a normal photoshock response. Therefore, the defect in this mutant is in a component critical for phototaxis, but one which is bypassed during photoshock. The PRC in *ptx3* is reduced approximately twofold, which is not enough to account for the very large defect in phototaxis. This indicates that the defect is downstream of the PRC, which may be affected indirectly. However, *ptx3* cells behave like wild type in EGTA, suggesting that the defect is upstream of the axoneme. One possibility is that *ptx3* has a defect in its ability to produce the hypothetical basal current in the

flagellum (see discussion of *ptx*2 and *ptx*8 above), precluding modulation of intraflagellar Ca^{2+} at submicromolar levels, and thereby completely eliminating phototaxis. In this case, a large depolarization would still open the voltage-sensitive flagellar Ca^{2+} channels and induce photoshock. The same defect might reduce the resting potential of the cell, indirectly affecting the size of the PRC. Additional electrophysiological studies of this mutant are in progress in an attempt to clarify the nature of its defect.

The fourth phenotypic class is made up of two alleles of *ptx*4. *ptx*4 cells have multiple misplaced eyespots and thus appear to be defective in the control of eyespot number and in the proper placement of the supernumerary eyespots. This is undoubtedly the cause of the phototaxis defect. Extra eyespots would send incorrect spatial information to the flagella, making the cell unable to track light and thus preventing phototaxis. In contrast, the direction of the stimulus is not important for photoshock, so this behavior is not affected by the loss of spatial information.

Certainly, additional mutants could be isolated that are defective in phototaxis and/or photoshock. Of the mutants characterized here, four (including *ptx*1) are represented by only a single allele, indicating that we have not yet saturated the phenotype. Moreover, we have not yet obtained mutants that have the phenotype expected for a defect in the genes encoding the photoreceptor molecule or the photoreceptor channel; it would be very interesting to have mutants of these classes. We also have not obtained mutants, such as the previously described *ey*1 (Hartshorne, 1953), in which the organization of the eyespot granules is disrupted under certain growth conditions (Morel-Laurens and Bird, 1984; Kreimer et al., 1992). Other mutants, such as *car*1 (Foster et al., 1984) and *lts*1 (CC2359; Iroshnikova et al., 1982; Lawson et al., 1991; Hegemann et al., 1991; Sineshchekov et al., 1994) have been described which have defects in carotenoid biosynthesis and thus are unable to produce the retinal cofactor needed for the photoreceptor. However, these latter mutants would not have been selected under our conditions of growth in light, because the defect either would not have been expressed (*car*1), or would have been lethal (*lts*1).

Because the defective loci in most of the new cell lines described here are tagged, it should be quite straightforward to clone the genes involved. Molecular characterization of these genes and their products will greatly advance our understanding of the signal transduction pathway for phototaxis and photoshock in *Chlamydomonas*. Moreover, since the insertional mutants are likely to be null, they will be very useful for detailed structural studies in which the cloned wild-type genes are altered by site-directed mutagenesis, and then introduced into the null mutants by transformation to determine how the alterations affect the functioning of the gene products. Thus, the mutants described here provide a foundation for elucidating the steps in a phototransduction pathway that, like those of vertebrate photoreceptor cells, is based on the cilium, and also for a molecular analysis of the individual components that function in this pathway.

We thank Dr. John Aghajanian and Ms. Christine Snay for expert assistance with the electron microscopy, Dr. Pete Lefebvre for the cloned *NIT*1 gene, Drs. Elizabeth Harris, Cynthia Horst, and Joel Rosenbaum for *Chlamydomonas* strains. We also thank Drs. Curtis Wilkerson, Cynthia Horst, Anthony Moss, Anthony Koutoulis, Pete Lefebvre, and John Larkin for helpful discussions.

This work was supported by National Institutes of Health grants GM14804 and GM30626; International Science Foundation grants NB600 and NB6300; and by funds from the International Center of the National Institutes of Health.

Received for publication 23 June 1995 and in revised form 26 July 1995.

References

Batschelet, E. 1981. Circular Statistics in Biology. Academic Press, London. 371 pp.

Bessen, M., R. Fay, and G. Witman. 1980. Calcium control of waveform in the isolated flagellar axonemes of *Chlamydomonas*. *J. Cell Biol.* 86:446–455.

Davis, T., M. Urdea, F. Masiarz, and J. Thorner. 1986. Isolation of the yeast calmodulin gene: calmodulin is an essential protein. *Cell.* 47:423–431.

Fernandez, E., R. Schnell, L. Ranum, S. Hussey, C. Silflow, and P. Lefebvre. 1989. Isolation and characterization of the nitrate reductase structural gene of *Chlamydomonas reinhardtii*. *Proc. Natl. Acad. Sci. USA.* 86:6449–6453.

Foster, K., and R. Smyth. 1980. Light antennas in phototactic algae. *Microbiol. Rev.* 44:572–630.

Foster, K., J. Saranak, N. Patel, G. Zarilli, M. Okabe, T. Kline, and K. Nakanishi. 1984. A rhodopsin is the functional photoreceptor for phototaxis in the unicellular eukaryote *Chlamydomonas*. *Nature (Lond.).* 311:756–759.

Gitelman, S., and G. Witman. 1980. Purification of calmodulin from *Chlamydomonas*: calmodulin occurs in cell bodies and flagella. *J. Cell Biol.* 87: 764–770.

Haga, N., M. Forte, R. Ramanathan, T. Hennessey, M. Takahashi, and C. Kung. 1984. Characterization and purification of a soluble protein controlling Ca^{2+}-channel activity in *Paramecium*. *Cell.* 39:71–78.

Harris, E. 1989. The *Chlamydomonas* Sourcebook. Academic Press, San Diego. 780 pp.

Hartshorne, J. 1953. The function of the eyespot in *Chlamydomonas*. *New Phyt.* 52:292–297.

Harz, H., and P. Hegemann. 1991. Rhodopsin-regulated calcium currents in *Chlamydomonas*. *Nature (Lond.).* 351:489–491.

Harz, H., C. Nonnengasser, and P. Hegemann. 1992. The photoreceptor current of the green alga *Chlamydomonas*. *Phil. Trans. R. Soc. Lond.* 338:39–52.

Hegemann, P., and B. Bruck. 1989. Light-induced stop response in *Chlamydomonas reinhardtii*: occurrence and adaptation phenomena. *Cell Motil. Cytoskeleton.* 14:501–515.

Hegemann, P., W. Gartner, and R. Uhl. 1991. All-*trans* retinal constitutes the functional chromophore in *Chlamydomonas* rhodopsin. *Biophys. J.* 60:1477–1489.

Hinrichsen, R., Y. Saimi, T. Hennessey, and C. Kung. 1984. Mutants in *Paramecium tetraurelia* defective in their axonemal response to calcium. *Cell Motil.* 4:283–295.

Hoops, H., and G. Witman. 1983. Outer doublet heterogeneity reveals structural polarity related to beat direction in *Chlamydomonas* flagella. *J. Cell Biol.* 97:902–908.

Horst, C., and G. Witman. 1993. *ptx*1, a nonphototactic mutant of *Chlamydomonas*, lacks control of flagellar dominance. *J. Cell Biol.* 120:733–741.

Huang, B., A. Mengersen, and V. Lee. 1988. Molecular cloning of cDNA for caltractin, a basal body-associated Ca^{2+}-binding protein: homology in its protein sequence with calmodulin and the yeast CDC31 gene product. *J. Cell Biol.* 107:133–140.

Iroshnikova, G., M. Rakhimberdieva, and N. Karaoetyan. 1982. Study of pigmentation-modifying mutations in strains of *Chlamydomonas reinhartii* of different ploidy. III. Characterization of disturbances of the photosynthetic apparatus in the presence of mutations in the *lts*1 locus. *Sov. Genet.* 18:1817–1824.

Kamiya, R., and G. Witman. 1984. Submicromolar levels of calcium control the balance of beating between the two flagella in demembranated models of *Chlamydomonas*. *J. Cell Biol.* 98:97–107.

Kindle, K. 1990. High-frequency nuclear transformation of *Chlamydomonas reinhardtii*. *Proc. Natl. Acad. Sci. USA.* 87:1228–1232.

Kreimer, G., C. Overlander, O. Sineshchekov, H. Stolzis, W. Nultsch, and M. Melkonian. 1992. Functional analysis of the eyespot in *Chlamydomonas reinhardtii* mutant *ey*627, *mt*−. *Planta.* 188:513–521.

Kuchka, M., and J. Jarvik. 1982. Analysis of flagellar size control using a mutant of *Chlamydomonas reinhardtii* with a variable number of flagella. *J. Cell Biol.* 92:170–175.

Kung, C. 1971. Genic mutants with altered system of excitation in *Paramecium aurelia*. II. Mutagenesis, screening and genetic analysis of the mutants. *Genetics.* 69:29–45.

Lawson, M., D. Zacks, F. Derguini, K. Nakanishi, and J. Spudich. 1991. Retinal analog restoration of phototactic responses in a blind *Chlamydomonas reinhardtii* mutant. *Biophys. J.* 60:1490–1498.

LeDizet, M., and G. Piperno. 1995. The light chain p28 associates with a subset of inner dynein arm heavy chains in *Chlamydomonas* axonemes. *Mol. Biol. Cell.* 6:697–711.

Levine, R., and W. Ebersold. 1960. The genetics and cytology of *Chlamydomonas*. *Annu. Rev. Microbiol.* 14:197–216.

Litvin, F., O. Sineshchekov, and V. Sineshchekov. 1978. Photoreceptor electric potential in the phototaxis of the alga *Haematococcus pluvialis*. *Nature (Lond.).* 271:476–478.

Melkonian, M., and H. Robenek. 1984. The eyespot apparatus of flagellated green algae: a critical review. *Prog. Phycol. Res.* 3:193–268.

Morel-Laurens, N., and M. Feinleib. 1983. Photomovement in an "eyeless" mutant of *Chlamydomonas*. *J. Photochem. Photobiol.* 37:189–194.

Morel-Laurens, N., and D. Bird. 1984. Effects of cell division on the stigma of wild-type and an "eyeless" mutant of *Chlamydomonas*. *J. Ultrastruct. Res.* 87:46–61.

Moss, A., G. Pazour, and G. Witman. 1995. Assay of *Chlamydomonas* phototaxis. *Methods Cell Biol.* 47:281–287.

Sager, R., and S. Granick. 1953. Nutritional studies with *Chlamydomonas reinhardtii*. *Ann. NY Acad. Sci.* 56:831–838.

Sambrook, J., E. Fritsch, and T. Maniatis. 1987. Molecular Cloning. Cold Spring Harbor Laboratory Press, Cold Spring Harbor, NY.

Seed, B. 1983. Purification of genomic sequences from bacteriophage libraries by recombination and selection *in vivo*. *Nucleic Acids Res.* 11:2427–2445.

Sineshchekov, O. 1991. Photoreception in unicellular flagellates: bioelectric phenomena in phototaxis. *In* Light in Biology and Medicine. Vol. II. R. H. Douglas, editor. Plenum Press, New York. 523–532.

Sineshchekov, O., E. Govorunova, A. Der, L. Keszthelyi, and W. Nultsch. 1992. Photoelectric responses in phototactic flagellated algae measured in cell suspension. *J. Photochem. Photobiol.* 13:119–134.

Sineshchekov, O., E. Govorunova, A. Der, L. Keszthelyi, and W. Nultsch. 1994. Photoinduced electric currents in carotenoid-deficient *Chlamydomonas* mutants reconstituted with retinal and its analogs. *Biophys. J.* 66:2073–2084.

Smyth, R., and W. Ebersold. 1985. Genetic investigation of a negatively phototactic strain of *Chlamydomonas reinhardtii*. *Genet. Res.* 46:133–148.

Taillon, B., S. Adler, J. Suhan, and J. Jarvik. 1992. Mutational analysis of centrin: an EF-Hand protein associated with three distinct contractile fibers in the basal body apparatus of *Chlamydomonas*. *J. Cell Biol.* 119:1613–1624.

Takahashi, M. 1979. Behavioral mutants in *Paramecium caudatum*. *Genetics.* 91:393–408.

Takeda, T., and M. Yamamoto. 1987. Analysis and in vivo disruption of the gene coding for calmodulin in *Schizosaccharomyces pombe*. *Proc. Natl. Acad. Sci. USA.* 84:3580–3584.

Tam, L., and P. Lefebvre. 1993. Cloning of flagellar genes in *Chlamydomonas reinhardtii* by DNA insertional mutagenesis. *Genetics.* 135:375–384.

Wilkerson, C., S. King, A. Koutoulis, G. Pazour, and G. Witman. 1995. The Mr 78,000 intermediate chain of *Chlamydomonas* outer arm dynein is a WD-repeat protein required for arm assembly. *J. Cell Biol.* 129:169–178.

Witman, G. 1990. Introduction to cilia and flagella. *In* Ciliary and Flagellar Membranes. R. Bloodgood, editor. Plenum Publishing Corp. 1–30.

Witman, G. 1993. *Chlamydomonas* phototaxis. *Trends Cell Biol.* 3:403–408.

Zacks, D., F. Derguini, K. Nakanishi, and J. Spudich. 1993. Comparative study of phototactic and photophobic receptor chromophore properties in *Chlamydomonas reinhardtii*. *Biophys. J.* 65:508–518.

Zimmer, W., J. Schloss, C. Silflow, J. Youngblom, and D. Watterson. 1988. Structural organization, DNA sequence, and expression of the calmodulin gene. *J. Biol. Chem.* 263:19370–19383.